TR-O-0131

30

Adaptive Selection of Oscillation Mode in a Chaotic Optical Ring to Avoid Collision

Yun Liu Peter Davis

1996. 3.15

ATR光電波通信研究所

Adaptive selection of oscillation mode in a chaotic optical ring to avoid collision

Yun Liu* and Peter Davis

ATR Optical and Radio Communications Research Laboratories

* Permanent address: Graduate School of Electronic Science and Technology, Shizuoka University, Johoku 3-5-1, Hamamatsu 432.

Contents:

I Introduction

In an optical chaos system which consists of a nonlinear optical resonator, the delay-induced self-oscillation exhibits multiple oscillation modes whose peak modulation patterns correspond to arbitrary bit sequences. Selection of oscillation mode, i.e. bit sequence, has been performed with various configurations, such like direct injection of specific signals, or adaptive feedback of the response signals. Recently, a novel method using adaptive chaotic phenomena has been proposed and experimentally tested by Davis et al.[1,2]

The target of current work is to build on the idea of adaptive mode selection using chaotic phenomena and propose a novel scheme for selection of output to avoid collisions with other periodic signals. This has potential application, for example, in an intelligent optical node which performs autonomous control of packet transmission schedules. An example of application of such adaptive mode selection is shown in Fig. 1.

II Experiment with Delayed Feedback System (DFS)

As schematically shown in Fig. 2, the DFS employed in the current experiment consists of a laser diode (λ=1.3 μm), an electrooptic intensity modulator (EOM), a single mode optical fiber delay line, and high-speed video amplifiers. The detailed configuration of the system is described in Appendix A. The time delay introduced by 1 km fiber is 5.2 μs and the response time of the system measures about 10 ns. In this system, harmonic modes up to 265 have been observed.[3] In the current experiment, we use 7th harmonic mode whose frequency reads 675 KHz. The top signals in Fig. 3 show examples of typical stable oscillation waveforms, with each peak level sequence corresponding to a periodic multi-bit sequence (in this case, a 7-bit binary sequence followed by the corresponding inverted 7-bit sequence, giving a periodic sequence of length 14-bits in Tim interval 4Tr, where Tr is the delay time in the ring).

A collision signal results from the output from the optical ring colliding with a periodic pulse sequence generated by an electrical pulse signal generator. The colliding operation is realized with another EOM. The optical signal from the optical ring is input to the EOM, and the electrical pulse sequence is applied to the electrical port of the modulator in such a way that the optical signal passes through the EOM only when the pulse is present. Then the collision signal corresponds to a high peak, or "1" in the optical output of the EOM. The collision signal is fed back with some arbitrary delay and injected into the ring.

Experiments with various collision signal periods and widths have been performed and results are summarized in Appendix B. Fig. 3 shows examples of sequence and collision signals before (Fig. 3a) and after (Fig. 3b) collision signal is fed back to drive adaptation. The oscillation in the ring adjusts so that the pulse no longer corresponds to a high peak, or "1" in the output. What makes this possible is chaotic fluctuations induced by the high peaks in the

feedback collision signal result in transitions among different oscillation patterns, corresponding to different 7-bit binary sequences. The feedback signal level is set by a variable attenuate so that the oscillation is stable unless there are high peaks in the feedback signal, which perturb, or kick as we call, the ring signal enough to induce chaotic transition to another sequence i.e. presence absence of collisions means presence/absence of chaotic transitions. The result of tuning chaos with kicks is further investigated and the details are shown in Appendix C.

III Experiment with Optical Chaos Memory (OCM)

Experimental setup for OCM is shown in Fig. 4. Here the nonlinear ring[4] has the similar configuration with the DFS. All the components have 3 dB bandwidths from DC to more than 3 GHz so one can obtain delay-induced oscillation in the GHz regime. We use 21st harmonic mode oscillation whose frequency is about 666 MHz. The light source employed in the nonlinear ring is a DFB laser diode (LD1) with the wavelength of 1553 nm.

The light output from the nonlinear ring is amplified by a fiber amplifier after a polarization controller. The amplified light signal is used as a control signal to gate another laser diode LD2 whose wavelength is 1549 nm. The control signal acts to suppress the intensity of the LD2 output. As reported by Davis et al,[5] by tuning the bias current, it is possible to obtain a thresholding effect whereby the LD2 only lases when the control signal is below a certain level. As a result, the light output of LD2 appears to be a binary sequence of light pulses corresponding to the intensity modulation of the control signal. It should be noted that the peaks in LD2 output correspond to the valleys of the control signal due to the suppression effect. The light output from LD2 is input into a tunable WDM through a 50:50 fiber coupler. The role of WDM is to select the signal of wavelength 1549 nm and remove signals of wavelength 1553 nm which are reflected by LD2. An LD amplifier is used to amplify the binary pulse and then deliver it to another fiber coupler which divides the pulse signal into two equal parts. One of them gets through a polarization controller to change its polarization direction and the other one gets through a fiber delay line. The basic idea is: for a fixed delay, different binary sequences have different collision signal patterns. So by choosing the delay time, one can get the optimum binary sequence that has the least collisions.

Some examples of experimental results are shown in Fig. 5. The top signals show 21st harmonic oscillation waveform of the output signal from nonlinear ring. The peak modulation of the oscillations from nonlinear ring corresponds to a bit sequence of "...11001100100110011...". The lower signal of Fig. 5(a) shows the light output of LD2. Since top and lower signals are not observed at the same point, the correspondence between two signals can not be directly recognized from the waveform. The lower signal of Fig. 5(b) is the same with (a) but with 2 m fiber delay line which results in 10.4 ns time delay. The lower

signal of Fig. 5(c) shows the overlap of two identical signals, i.e. two signals without time delay between them, while the lower signal of Fig. 5(d) shows the collision of (a) and (b). Unlike Fig. 5(c) which has the same pattern with original ones, the high peak distribution pattern in Fig. 5(d) is dependent to the delay time between two original signals. Such high peaks are results of collision of two signals. By feeding back this collision signal into OCM and appropriately setting the bias of EOM and LD1, the high peaks can kick the system into chaotic region and generate different oscillation patterns until an optimum oscillation pattern that results in less high peaks in the collision signal is found.

The main problem is the interference of two bit sequences. Even a polarization controller is introduced in one of the optical paths to avoid interfering, polarization direction fluctuates due to subtle variations of temperature, etc. The interference results in fluctuations in the collision signal. To obtain a stable feedback signal and better performance of mode selection, generation of collision signal without any interference is required. This can be implemented by colliding two signals of different wavelength, e.g. signals of nonlinear ring and LD2, but with definite phase relations. The experiment is now in proceeding.

IV Video Visualization of Spatio-temporal Chaos

It is well known that chaos in a nonlinear ring with time delay can be described with a delay-differential equation and such kind of dynamics has two-fold property.[6] One is its discrete feature: there is a nonlinear mapping between states if one viewing the time development of the output in stroboscopic way with the sampling width equal to the delay time; The second feature is the continuity: the current state relates its neighboring states through the differential term. Therefore, the delay induced chaos can be visualized in a spatio-temporal version. Here "space" means the state within the delay and "time" means the discrete step of delay. Recently, such spatio-temporal visualization has been performed on a computer display where chaotic time sequences have been shown to correspond to different patterns including cellular automaton.[7]

Since the delay time in the DFS system is about 5.2 μs, it is possible to visualize the time series on a TV display whose HD line period is 63.5 μs. The key point is how to synchronize the output signal to TV. We obtain the frame pulse from the output signal and then input the frame pulse to a function generator as a synchronization signal. The output of the function generator is set as the VD line signal (without interleave) of TV and synchronize another function generator to generate HD line signal. Detailed setup can also be found in Appendix A.

Fig. 6 shows the pattern of one 7th harmonic mode oscillation whose peak modulation pattern corresponding to a bit sequence of "...1110111...". The bit sequence can be directly read

from the stripe distribution pattern. When the system evolves into chaotic region, some interesting phenomena are observed. Fig. 7 shows an example for chaotic output which appears to be a type of cellular automata. This is the first time to demonstrate a real-time formation of cellular automata with delay-induced chaos. It is not strange to observe automata with delay-induced chaos. All of conditions for the generation of automaton[8] are satisfied in the delayed nonlinear ring: discrete time (in unit of delay), discrete space (in unit of response time or time resolution of TV), discrete state (gray level resolution of TV), neighboring spatio-temporal relations have been readily realized by discrete-differential property of delay-induced chaos.

References

[1] P. Davis, *Jap. Journ. Appl. Phys.* **29** (1990) L1238.

[2] T. Aida, P. Davis, *IEEE J. Quantum Electron.*, **30** (1994) 2986.

[3] T. Aida, P. Davis, *IEEE J. Quantum Electron.*, **28** (1992) 686.

[4] T. Aida and P. Davis, *Technical Digest of CLEO/Pacific Rim 95*, (1995) 118.

[5] P. Davis and R. Helkey, *Technical Digest of CLEO/Pacific Rim 95*, (1995) 118.

[6] K. Ikeda and K. Matsumoto, *Physica D* **29** (1987) 223.

[7] F. T. Arecchi, G. Giacomelli, A. Lapucci, and R. Meucci, *Phys. Rev. A* **45** (1992) R4225.

[8] S. Wolfram (ed.), *Theory and Applications of Cellular Automata*, World Scientific, 1986.

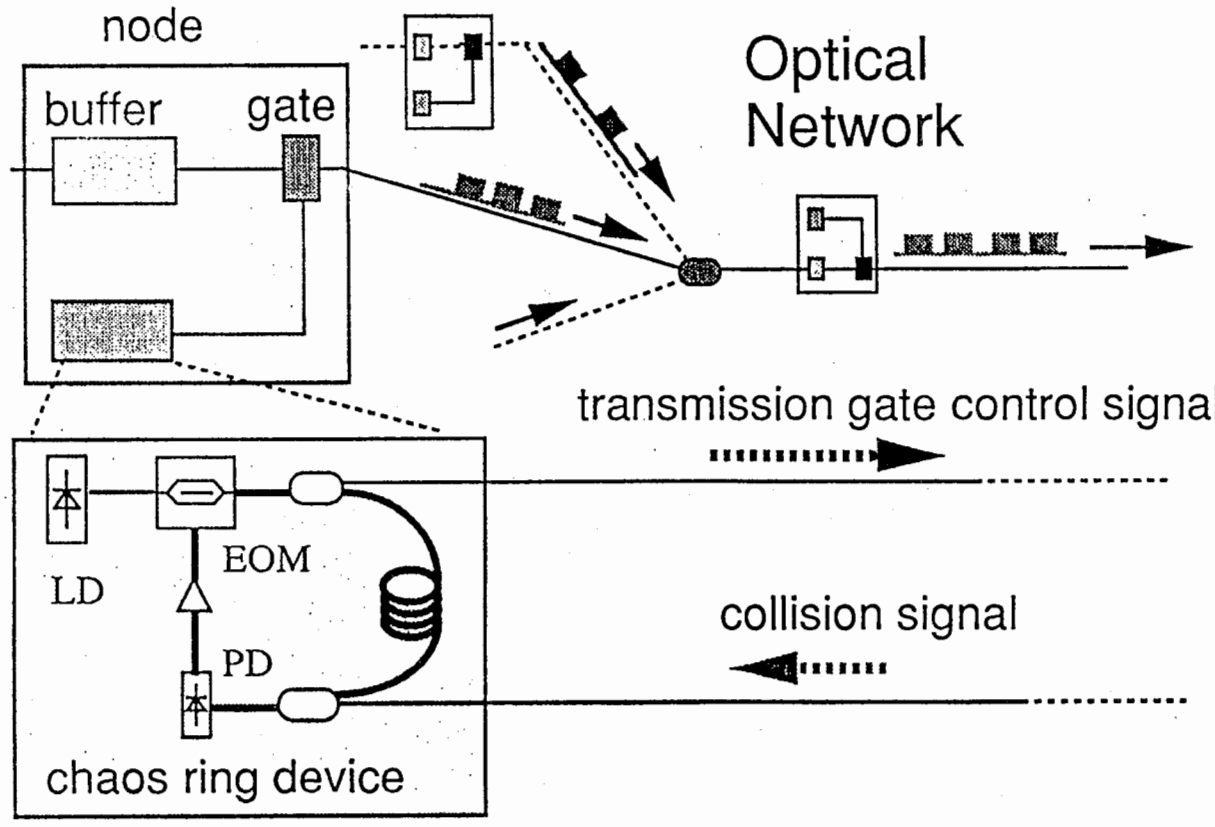

Fig. 1 Chaotic device generating signals to control packet transmission. Collision driven chaotic mode search results in avoidance of output collisions.

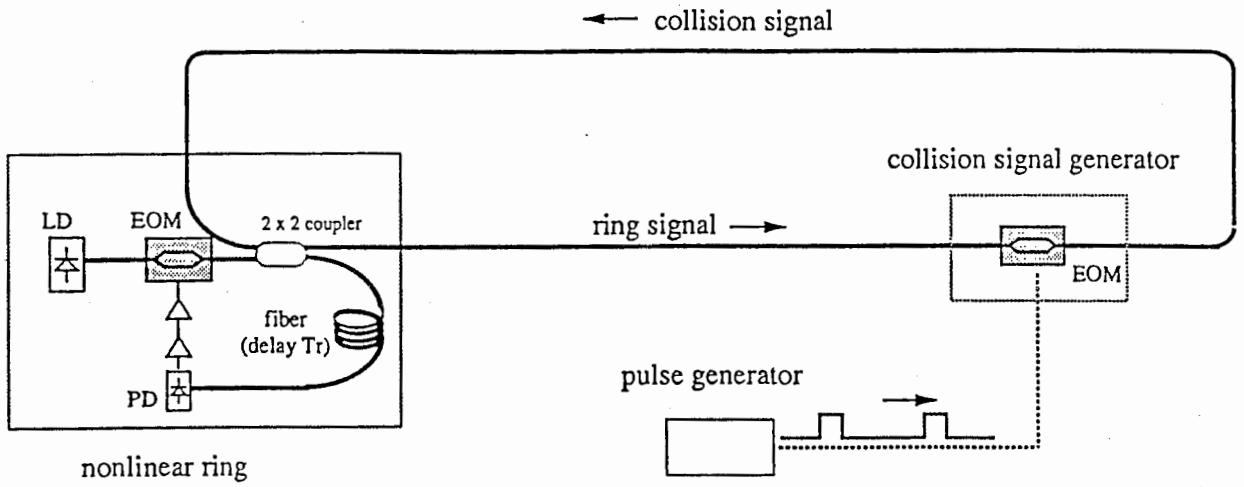

Fig. 2 Experimental scheme for adaptation to avoid output collision.

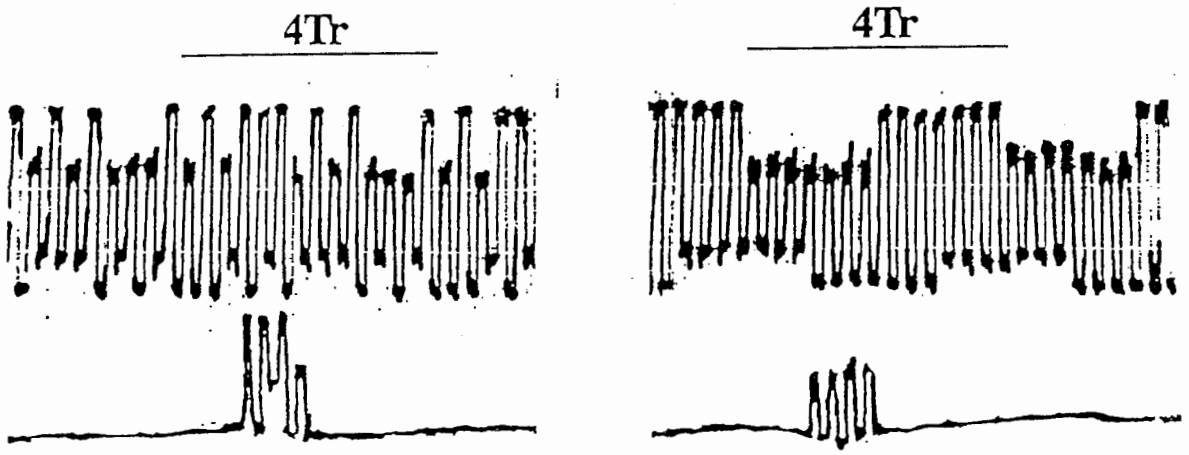

(a) before adaptation (b) after adaptation

Fig. 3 Examples of oscillating ring output (top) and collision signals (lower) before and after adaptation. (a) before adaptation, pulse coincides with "1101" peak sequence, (b) after adaptation, pulse coincides with "0000" peak sequence.

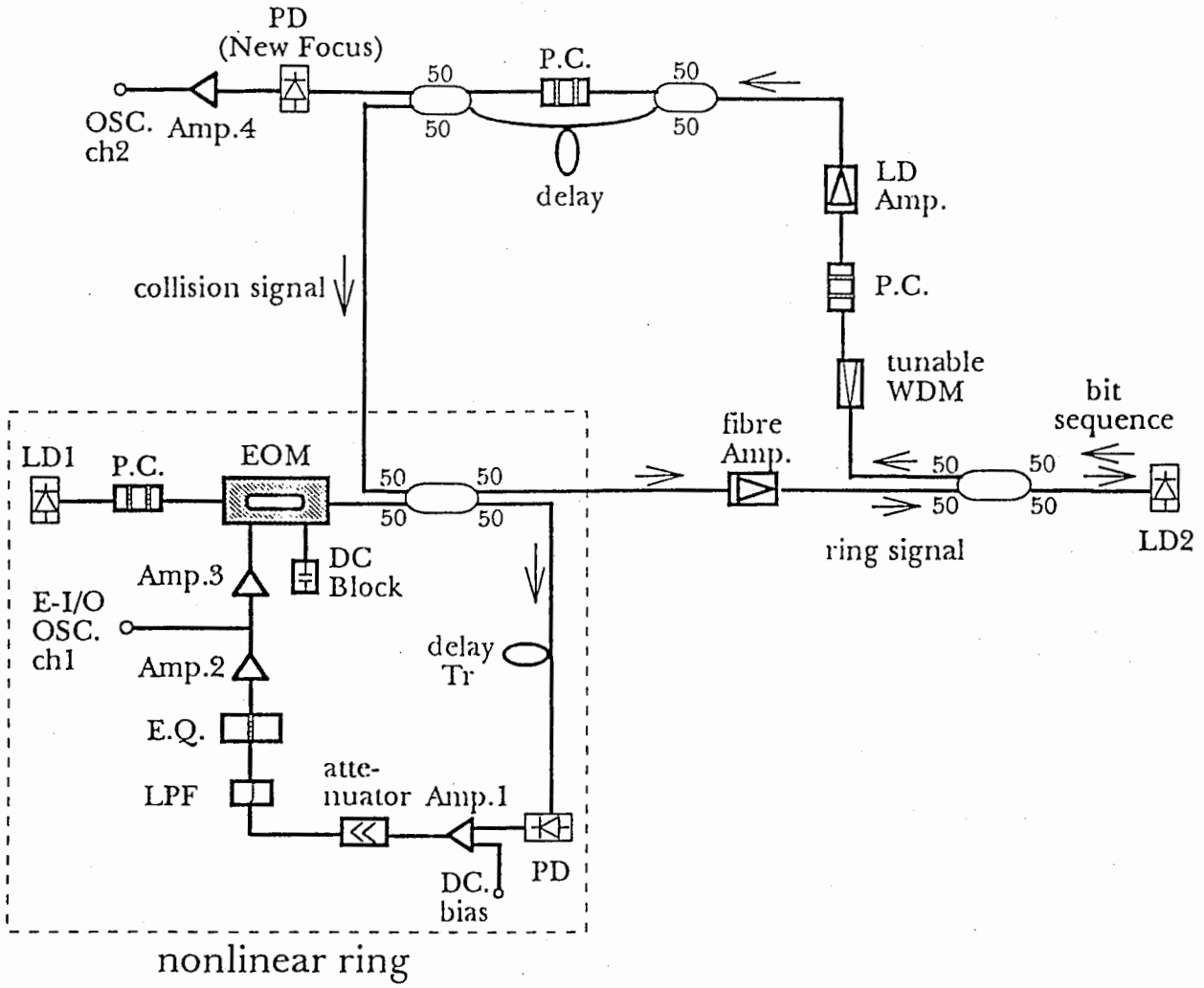

LD:	λ=1553 nm
LD2:	λ=1549 nm, I_b=19.2 mA, 25℃
P.C.:	Polarization Controller
Fibre Amp.:	ErFA-1110, I_b=200 mA
LD Amp.:	Anritsu SD3A10P2, LD driver, I_b=148 mA, 25℃
Amp.4:	B&H AC7020H

Fig. 4 Experimental setup with OCM

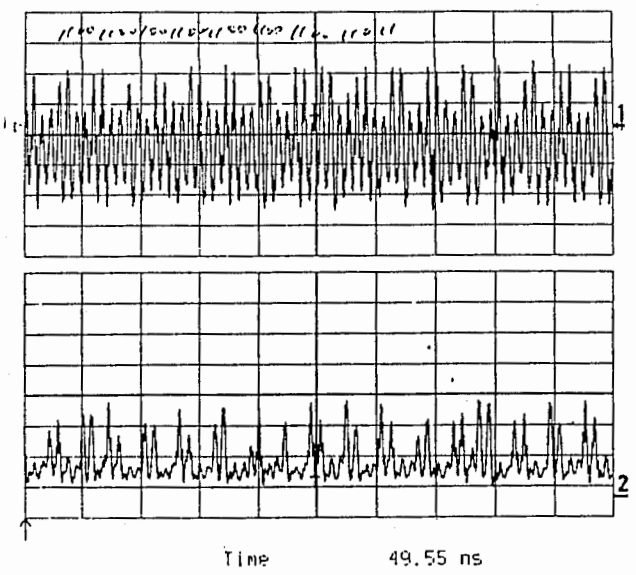

Fig. 5(a) 21st harmonics (top) and its bit sequence with no extra time delay introduced (lower).

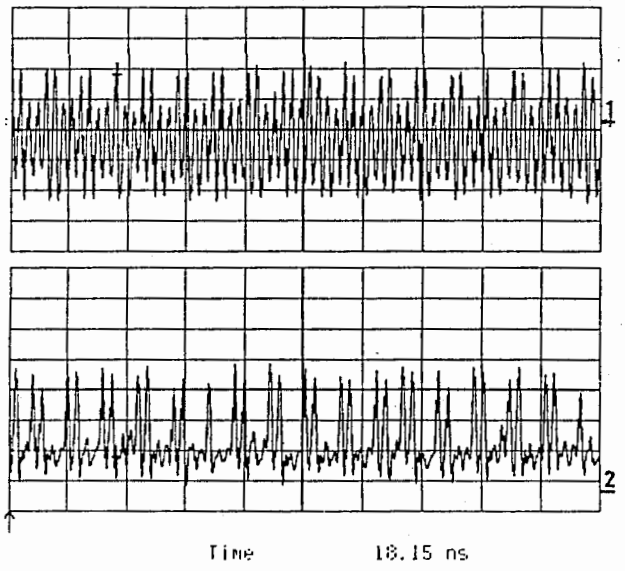

Fig. 5(b) 21st harmonics (top) and its bit sequence with 10.4 ns time delay (lower).

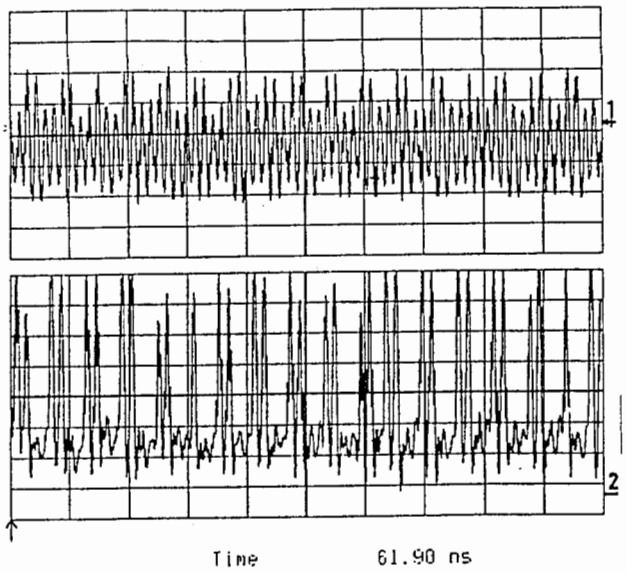

Fig. 5(c) Overlap of two identical signals.

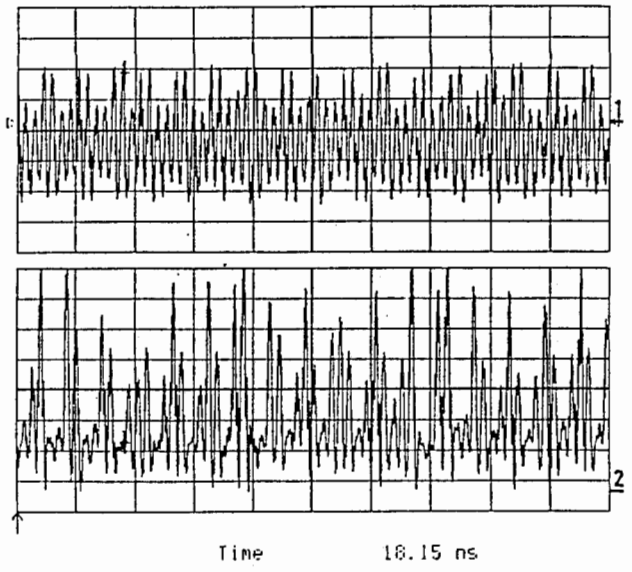

Fig. 5(d) Collision of (a) and (b).

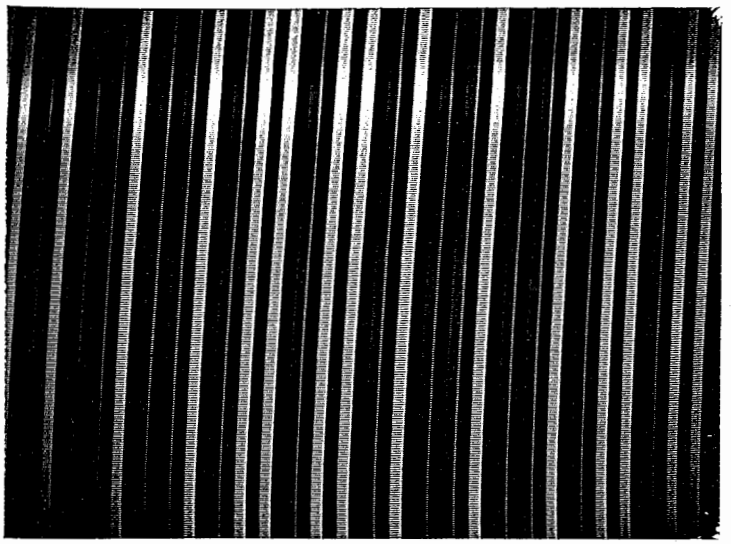

Fig. 6a Video visualization of 7th harmonic mode oscillation

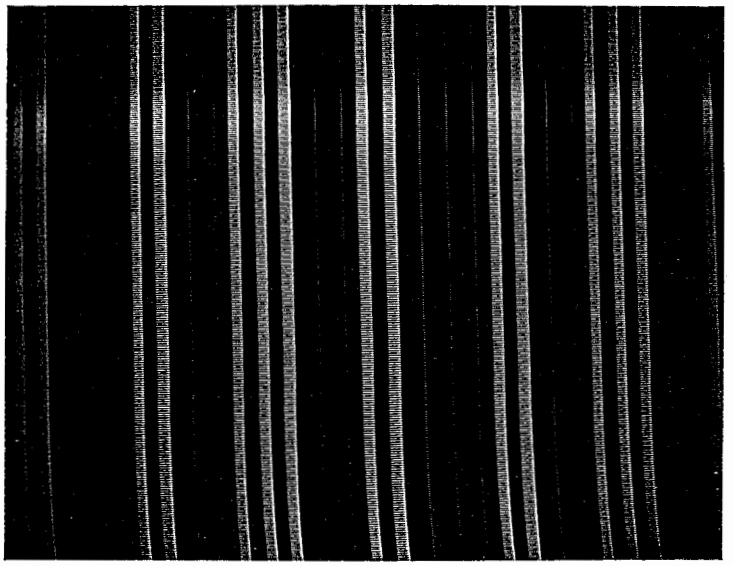

Fig. 6b Video visualization of 7th harmonic mode oscillation

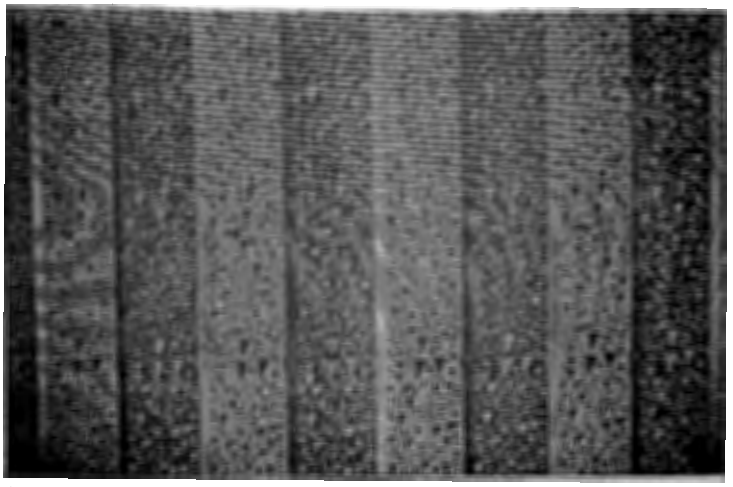

Fig. 7 Video visualization of chaos (fundamental harmonic mode chaos)

Appendix A Detailed Setup for Experiment with DFS.

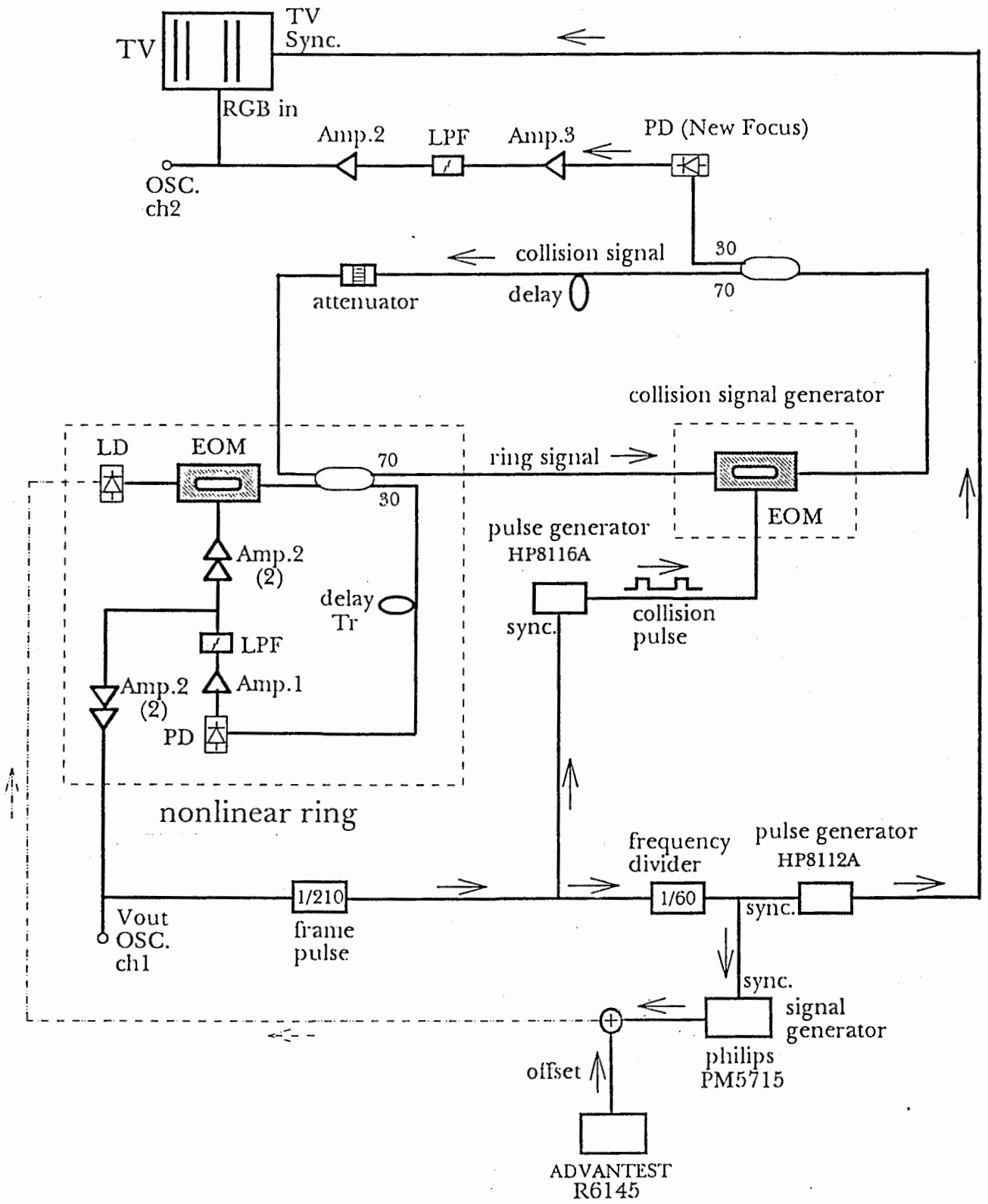

Fig. A-1 Experimental setup for DFS.

Some notations for Fig. A–1

Amp.1: Combinear, 20 dB, Invert
Amp.2: Combinear, 20 dB, Non–invert
Amp.3: SA230F5, 46 dB

TV Syncronizing singal: T=63.3～63.5 μs, Amplitude ±0.9V, duty ratio 80%～94%.
Pulse Generator HP8112A

Trigger Mode:	Gate	
Slope:	–	

Collision pulse: f=47.9～48.1 KHz (4 Tr), 9.53～9.57 KHz(20 Tr), Amplitude +0.1V～–2.0 V, pulse width 3.0～6.5 μs (2～5 bits)
Pulse Generator HP8116A

Trigger Mode:	Gate	
Slope:	–	for cases of 4 Tr and 20 Tr
Trigger Mode:	normal	
Slope:	–	for the case of 60 Tr

Signal Generator philips PM5715

Period = trigger period (～18 ms)
Amplitude: 50～100 mV
Offset: adjustable
Duty Ratio: 50%

ADVANTEST R6145

DC bias generator

LD input voltage: –3.615 ～ –3.695 V for the bifurcation range from $\xi_{2,7}$ mode to chaos

Operating harmonics: 7th harmonic, period=1.5 μs.

Appendix B Success Rate for Different Collision Periods and Widths

We made a statistical evaluation of the success rate of adaptive mode selection with DFS. To do this, we modulate the bias current of laser diode in DFS (see Fig. A-1) with a low-frequency square wave signals. High and low levels of the modulation signal is chosen in such a way that the nonlinear ring can be induced to chaotic transition by high peaks in the feedback signal within the low level interval, but stays at chaos region within high level interval in regardless of the feedback signal. Therefore, we can repeat the trial of mode selection for many times and make statistical measurements. One of measurements is to investigate the success rate of the mode selection within the time interval of the modulation period. The following results are obtained with the modulation signal period of 9 ms that is about 1800 times of the delay time. We have made investigations for three different collision periods (4 T_r, 20 T_r, and 60 T_r) and three different collision signal width (2 bits, 3 bits, and 4 bits). Here, one bit means one pulse of 7th harmonic mode oscillation, i.e. 1.5 μs. For each pair, we investigated two feedback cases: direct feedback and feedback with arbitrary time delay. It turns out that collision signal period of 20 T_r is most effective for adaptive chaotic search.

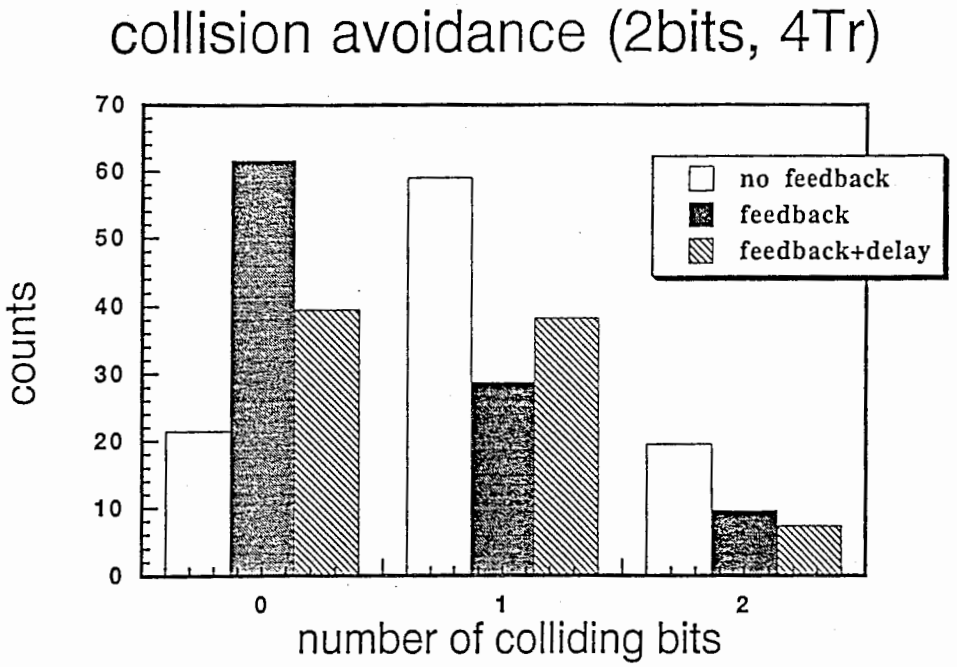
collision avoidance (2bits, 4Tr)
70
60
50
40
30
20
10
0
counts
0
1
2
number of colliding bits
no feedback
feedback
feedback+delay

Fig. B-1

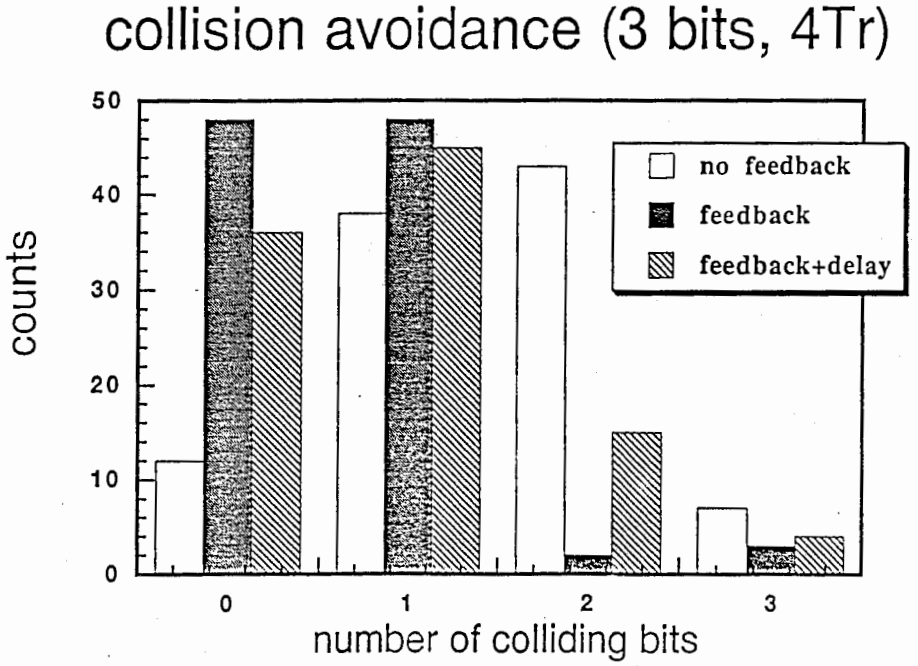
collision avoidance (3 bits, 4Tr)
50
40
30
20
10
0
counts
0
1
2
3
number of colliding bits
no feedback
feedback
feedback+delay

Fig. B-2

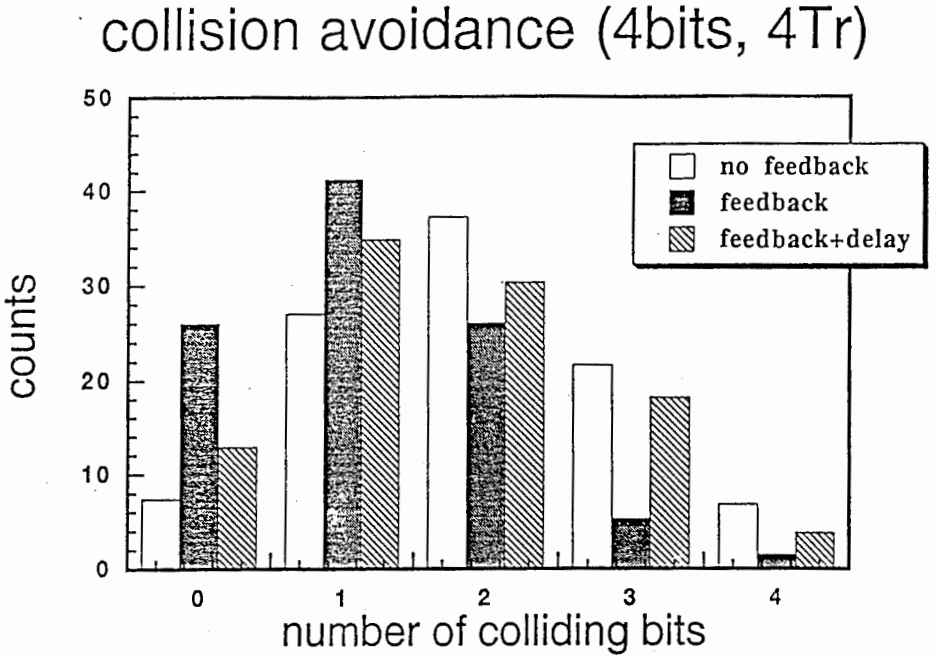
collision avoidance (4bits, 4Tr)
50
40
30
20
10
0
counts
0
1
2
3
4
number of colliding bits
no feedback
feedback
feedback+delay

Fig. B-3

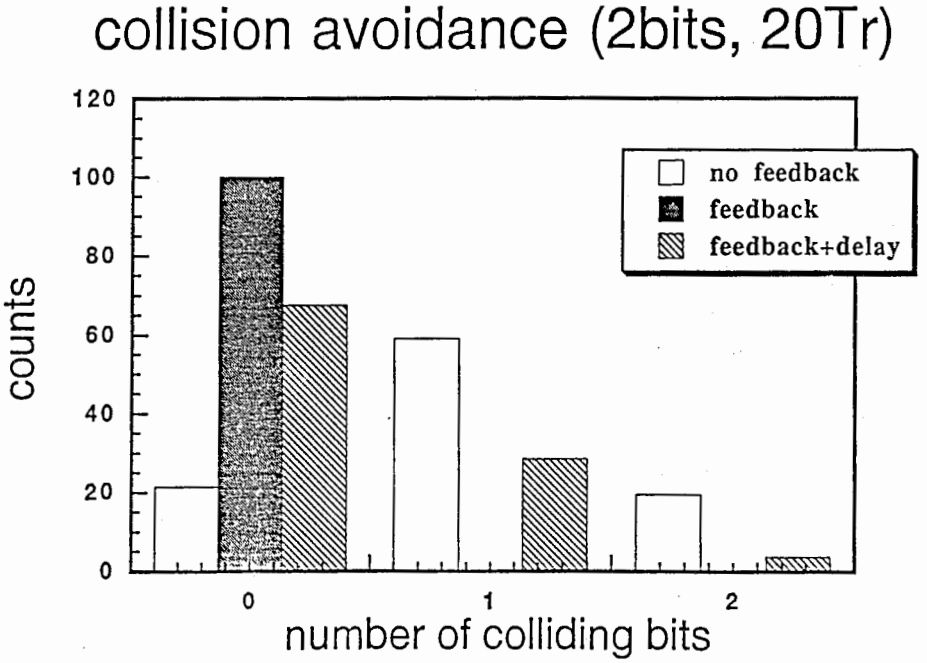
collision avoidance (2bits, 20Tr)
120
100
80
60
40
20
0
counts
0
1
2
number of colliding bits
no feedback
feedback
feedback+delay

Fig. B-4

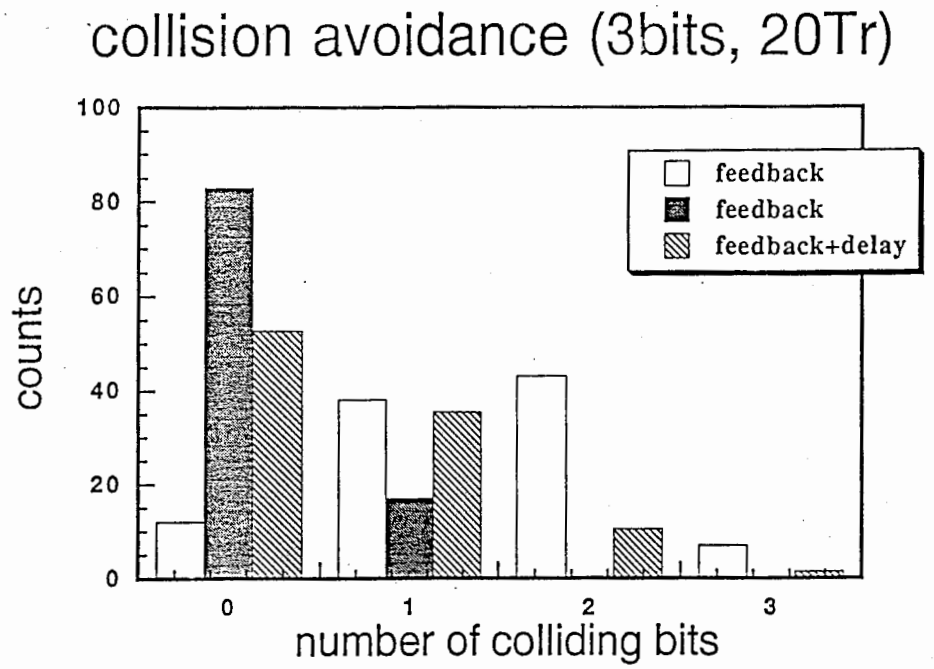
collision avoidance (3bits, 20Tr)
100
80
60
40
20
0
counts
feedback
feedback
feedback+delay
0
1
2
3
number of colliding bits

Fig. B-5

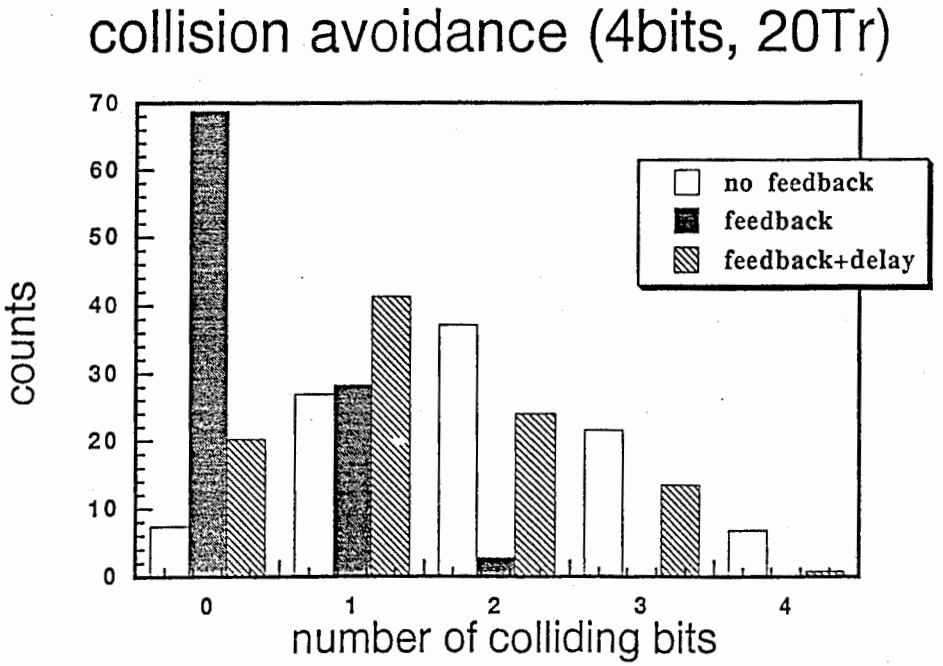
collision avoidance (4bits, 20Tr)
70
60
50
40
30
20
10
0
counts
no feedback
feedback
feedback+delay
0
1
2
3
4
number of colliding bits

Fig. B-6

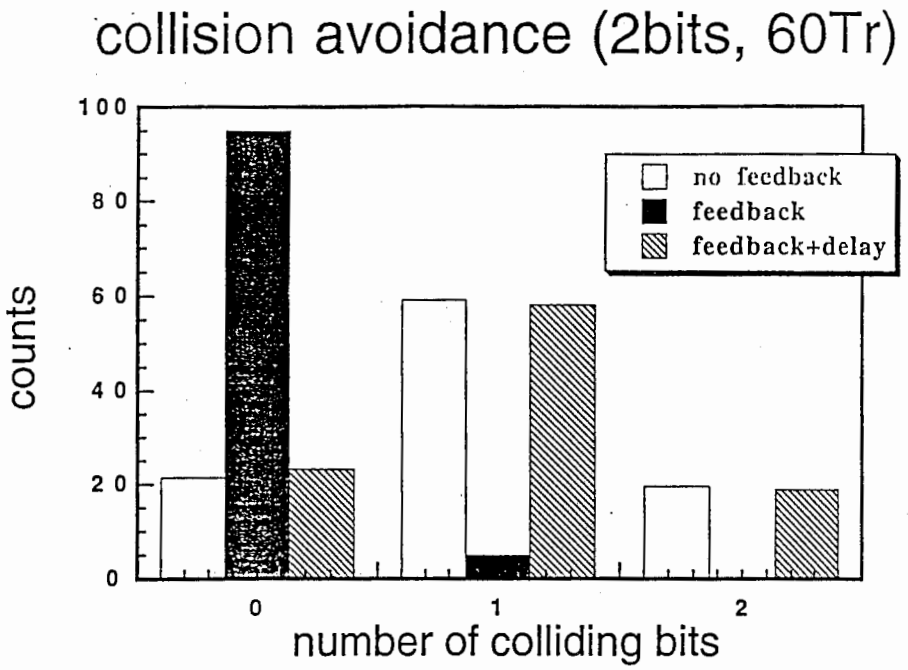
collision avoidance (2bits, 60Tr)
100
80
60
40
20
0
counts
no feedback
feedback
feedback+delay
0
1
2
number of colliding bits

Fig. B-7

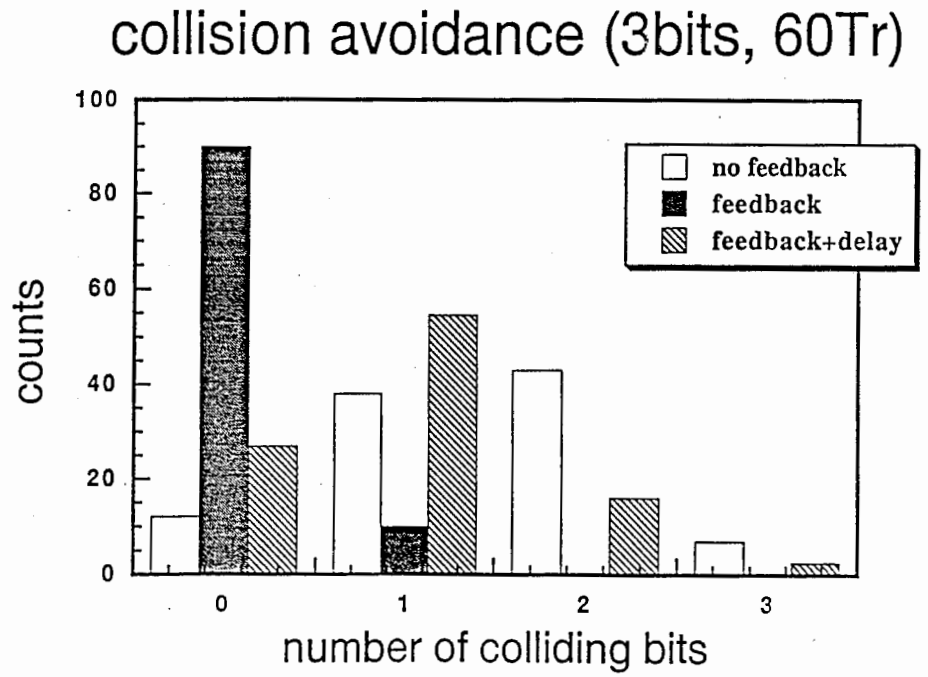
collision avoidance (3bits, 60Tr)
100
80
60
40
20
0
counts
no feedback
feedback
feedback+delay
0
1
2
3
number of colliding bits

Fig. B-8

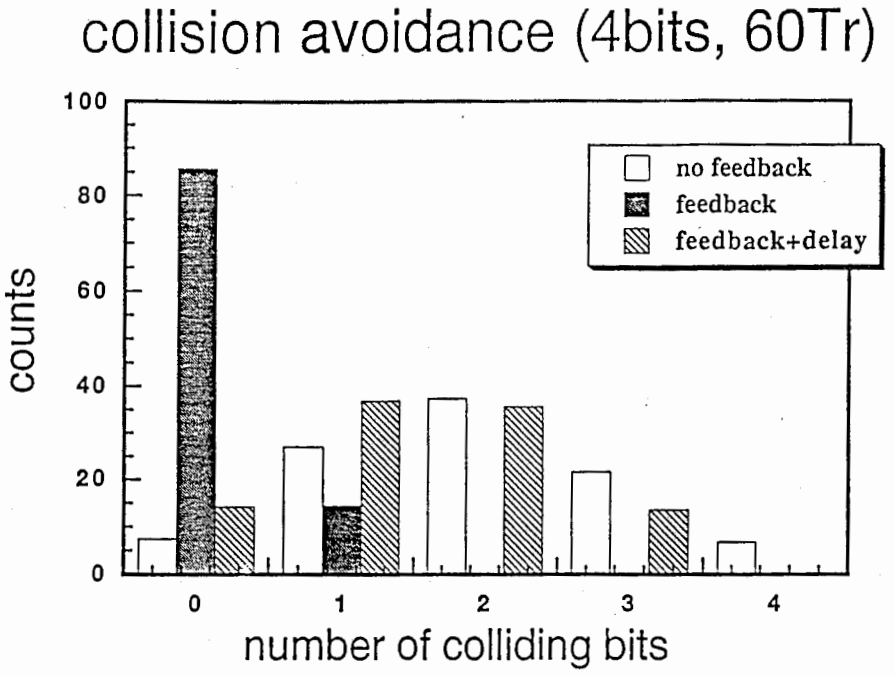
collision avoidance (4bits, 60Tr)
100
80
60
40
20
0
counts
0
1
2
3
4
number of colliding bits
no feedback
feedback
feedback+delay

Fig. B-9

Appendix C Tuning Chaos with Kicks

Unlike previous methods of chaotic search where continuous feedback signal is applied to the system's control parameter to induce chaos, the feedback in the experiment with DFS uses only a small part of collision signal (high peaks). As described in Section II, such high peaks kicked the system into chaotic transition and leaded to successful mode selection although the mode search time is longer than continuous feedback case. To verify the effect of tuning chaos with kicks, we investigate the open loop behavior by directly applying to the bias of EOM with periodic pulses. The result for the period of 20 T_r (104 μs) is plotted in Fig. C–1. Transversal axis indicates the pulse width while ordinate axis indicates critical power (measured with power meter) for the onset of chaos from a pre–chaos state. To compare with continuous feedback, the critical power is normalized to that of the continuous feedback. For pulse width narrower than T_r (5.2 μs), the critical power remains unchanged which means that as long as pulse amplitude is strong enough, pulse width is not important to induce chaos. On the other hand, when pulse width is wider than $2T_r$ (10.4 μs), the critical power is proportional to the pulse width. This implies that only pulse amplitude works when the pulse width exceeds 2 T_r.

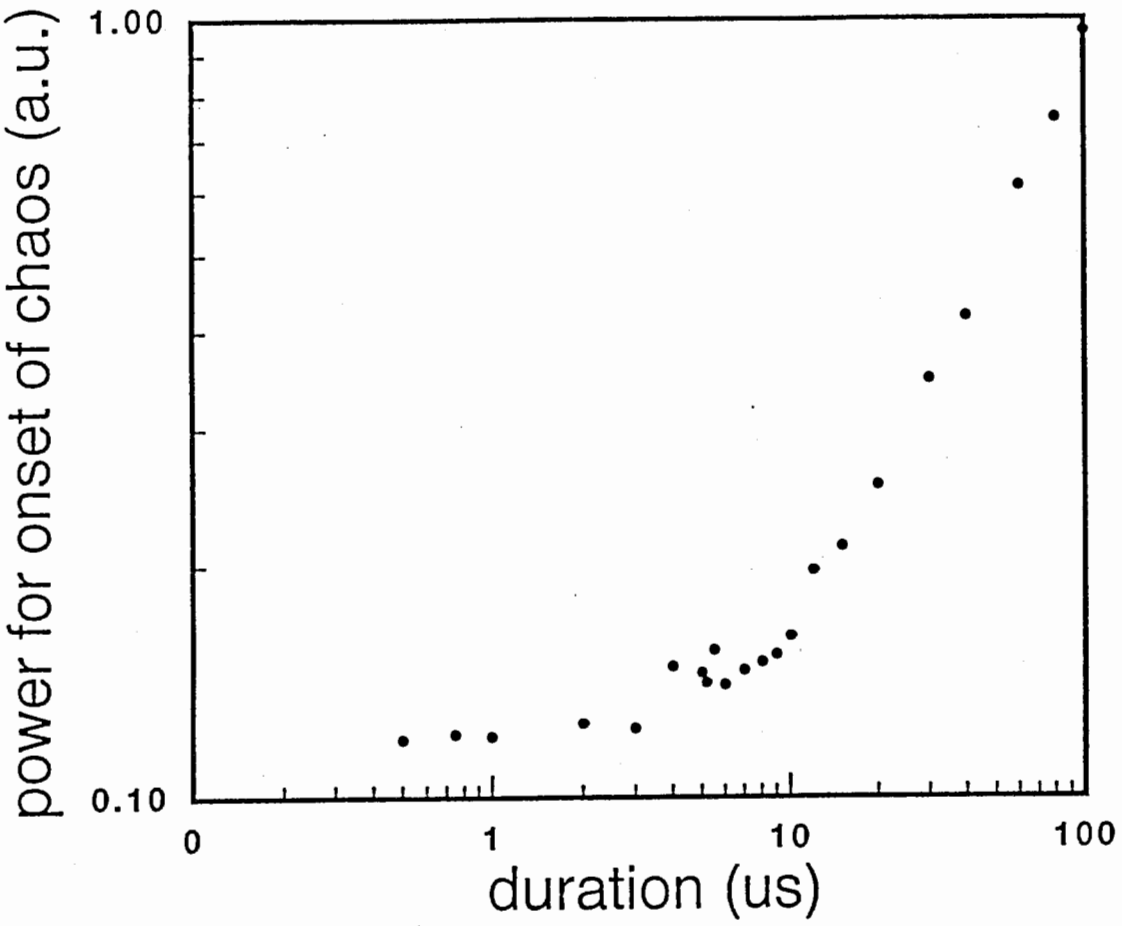

Fig. C-1 Open loop behavior of tuning chaos with kichs. (pulse period T=20 T_r =104 μs, critical power is normalized to the value of critical power for continuous feedback, i.e. pulse width =T)